Short communication

Surface quality and mechanical property evolution of laser nitrided Zr-based metallic glass induced by laser shock flattening

Hu Huang [a], Puhong Xu [a], Bo Liu [a], Hong An [a], Yongfeng Qian [a,*], Jiwang Yan [b]

[a] Key Laboratory of CNC Equipment Reliability, Ministry of Education, School of Mechanical and Aerospace Engineering, Jilin University, Changchun, 130022, China
[b] Department of Mechanical Engineering, Faculty of Science and Technology, Keio University, Yokohama, 223-8522, Japan

ARTICLE INFO

ABSTRACT

Laser nitriding is an effective modification technique to improve the comprehensive mechanical properties of metallic glasses (MGs). However, numerous micro-defects, such as pores and humps, usually appear on the laser-nitriding-treated (LNed) MG surface, and therefore additional post-treatment is required. Herein, laser shock processing was implemented to flatten the LNed MG and as well modify its surface mechanical property. The dependence of the laser shock flattening process on the laser energy density was investigated. The results revealed that the surface micro-defects on the LNed MG were significantly reduced after laser shock flattening, and accordingly, the surface roughness (Sa) was decreased, with a maximum reduction of 61.87% (from 0.48 to 0.183 μm) achieved at a relatively high laser energy density of 178.3 J/cm^2. Furthermore, nanoindentation measurements indicated that although the surface hardness of the LNed MG was decreased after laser shock flattening, it was still higher than that of the as-cast MG.

1. Introduction

Laser nitriding (LN) is a highly effective strategy in improving the surface mechanical properties of Zr-based metallic glasses (MGs) [1], by which a high-hardness metallurgical bonded nitrided layer with a thickness of tens or even hundreds of microns can be formed within seconds [2,3]. However, complicated interactions between the incident laser beam, laser-induced high-temperature and high-pressure plasma, MG target and nitrogen gas occur during the laser surface nitriding process, and this extreme non-steady condition usually results in non-uniform deformation of the melt pool on the MG surface [4], i.e., degradation of the surface quality. As reported in a previous study [2], by nanosecond laser irradiation in a flowing nitrogen atmosphere, a high-hardness nitrided layer was formed on the MG substrate. Unfortunately, accompanied by this nitriding process, numerous micro-defects, such as humps, dents, and micro-sized particles, were simultaneously generated on the laser-nitriding-treated (LNed) MG surface. The question then arises to whether there is an effective post-treatment strategy that can enhance the surface quality of the LNed MGs and thus broaden their applicability in practical engineering.

Conventional mechanical polishing is obviously not suitable for treating LNed MG due to its high hardness, while other well-established polishing techniques such as electrochemical polishing [5,6], chemical polishing [7,8], ultrasonic vibration-assisted polishing [9,10], and ion beam thinning [11,12] also have some limitations such as non-environmental friendliness and cumbersome operation steps. Compared to the polishing methods mentioned above, the laser shock flattening technique offers additional advantages, such as localized treatment, limited substrate thermal deformation, non-contact, and ultra-high shock pressure [13–17], which makes it highly promising for achieving surface flattening of various metal parts [18], especially for metal foils [19]. However, in contrast to the well-established processing principle and cutting-edge understanding of laser shock flattening of crystalline metals, the fundamental understanding of laser shock flattening of LNed MG remains in its vacancy.

Herein, the LNed MG surface was subjected to laser shock flattening at different laser energy densities, especially focusing on the investigation of surface quality and mechanical property evolution as well as the physical origin underlying such changes. The results revealed that the surface micro-defects on the LNed MG were significantly reduced after laser shock flattening, leading to a considerable enhancement of the surface quality. More importantly, although the surface hardness of the LNed MG was decreased after laser shock flattening, it was still higher than that of the as-cast MG. This study provides an ideal solution for

* Corresponding author.
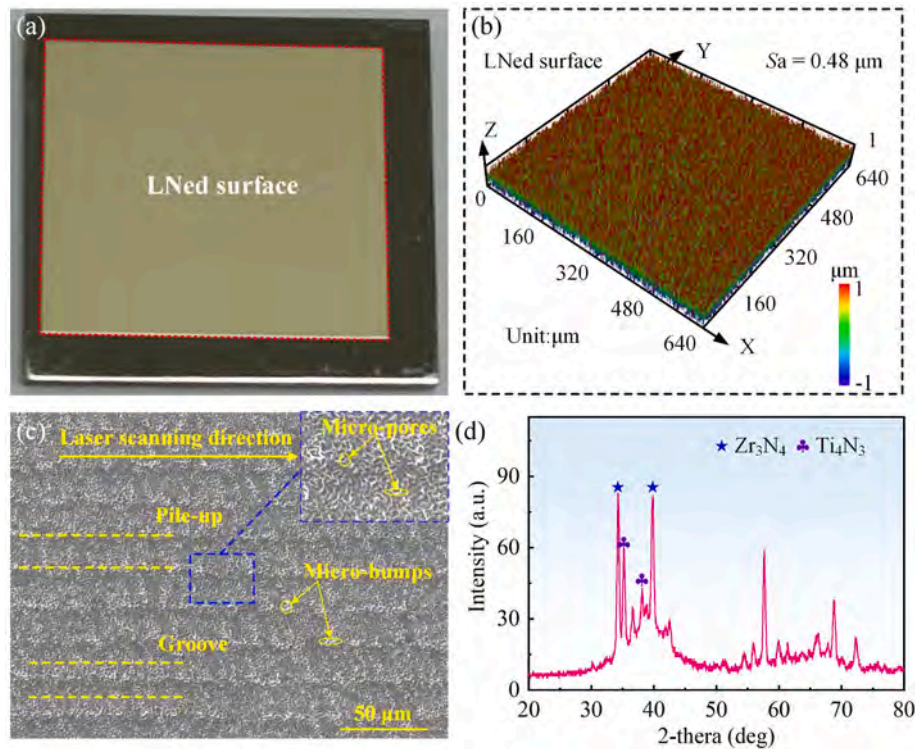 E-mail address: qianyf@jlu.edu.cn (Y. Qian).

Fig. 1. Macro and micro characterization of the LNed MG surface: (a) macroscopic photograph, (b) 3D topography, (c) SEM morphology, and (d) XRD spectrum.

improving the surface quality of the LNed metal parts.

2. Materials and methods

A commercial Zr-based MG plate (20 mm × 20 mm × 2 mm) with a composition of $Zr_{41.2}Ti_{13.8}Cu_{12.5}Ni_{10}Be_{22.5}$ (at.%) was used as raw material. Prior to LN treatment, the MG sample was mechanically polished to a mirror finish, with a surface roughness of about 4 nm. The LN experiment was implemented using a nanosecond pulsed laser system that was controlled by a computer. This system was configured with a fiber laser (SP–050P-A-EP-Z-F-Y, SPI Lasers) running at a wavelength of 1.064 μm, possessing a spot diameter of approximately 43 μm and a Gaussian energy distribution. Based on our previous investigation [2], the optimized LN conditions were set as follows: laser power of 11.4 W, scanning speed of 40 mm/s, overlap rate between adjacent laser irradiation lines of 95%, and nitrogen pressure of 0.01 MPa.

After LN treatment, the resulting LNed MG surface was subjected to laser shock flattening by a self-developed laser shock processing system equipped with a Q-switched Nd:YAG laser (SpitLight 2000, laser wavelength $\lambda = 1064$ nm, repetition frequency $f = 1$ Hz, pulse width $t_p = 8$ ns, focus diameter $d = 1$ mm, and flat-top energy distribution). To investigate the dependence of the laser shock flattening process on the processing conditions, five laser energy density levels of 76.4, 101.9, 127.3, 153.8, and 178.3 J/cm² were selected, corresponding to five test cases. To avoid oxidation, all laser shock flattening experiments were performed in a pure argon environment. In addition, no protective or confining layer was utilized during the laser shock flattening process to avoid cumbersome pre-treatment and post-treatment process.

To explore the changes in surface characteristics induced by laser shock flattening, the surface morphology and topography of the LNed MG and five test cases were characterized by a scanning electron microscope (SEM, JSM-IT500A, JEOL) and a laser scanning confocal microscope (LSCM, OLS4100, Olympus). The chemical compositions of the studied MGs were determined by using a X-ray diffractometer (XRD, D8 Advance) and an energy dispersive X-ray spectrometer (EDS, EX-74600U4L2Q, JEOL). The surface hardness of the LNed MG and five test cases was determined using a nanoindentation instrument (DUH-211S, Shimadzu) with indentation load of 150 mN, loading rate of 10 mN/s, and holding time of 5 s.

3. Results and discussion

Fig. 1(a) presents the macroscopic photograph of the MG sample after LN treatment, in which the square LNed region exhibits a yellowish brown color that is clearly differentiated from the MG substrate, which is consistent with the results reported in the literature [2]. Fig. 1(b) provides the three-dimensional (3D) topography corresponding to the LNed region shown in Fig. 1(a), from which it is seen that the LNed region is covered with dense micro-bumps and possesses a surface roughness (*Sa*) of 0.48 μm, implying that the MG sample underwent significant thermal deformation during the LN process. Meanwhile, from the SEM morphologies illustrated in Fig. 1(c), some parallel pile-ups and grooves covered with a large number of micro-bumps and micro-pores along the laser scanning direction emerge on the LNed surface. The formation of these micro-bumps and micro-pores during the LN process is mainly attributed to the thermal expansion and vapourization of the MG and unstable melt flow with the action of driving forces such as the Marangoni force and recoil pressure [20]. In addition, the significant differences in the physical properties of the in-situ formed nitrided phases and the MG substrate further contribute to the generation of these micro-defects. Fig. 1(d) presents the XRD spectrum of the LNed MG, from which multiple sharp diffraction peaks are observed, and the dominant diffraction peaks can be well indexed as Zr_3N_4 and Ti_4N_3 crystalline phases.

Fig. 2(a)-(e) presents the SEM morphologies and corresponding 3D topographies of the LNed surface after laser shock flattening under different laser energy densities, corresponding to five test cases. By comparing the surface morphology of the LNed MG and five test cases, it is concluded that the LNed regions become smoother after laser shock flattening, which can be attributed to plastic deformation induced by high pressure produced by the laser shock wave. In addition, the evident changes from case 1 to case 5 are that micro-defects including micro-
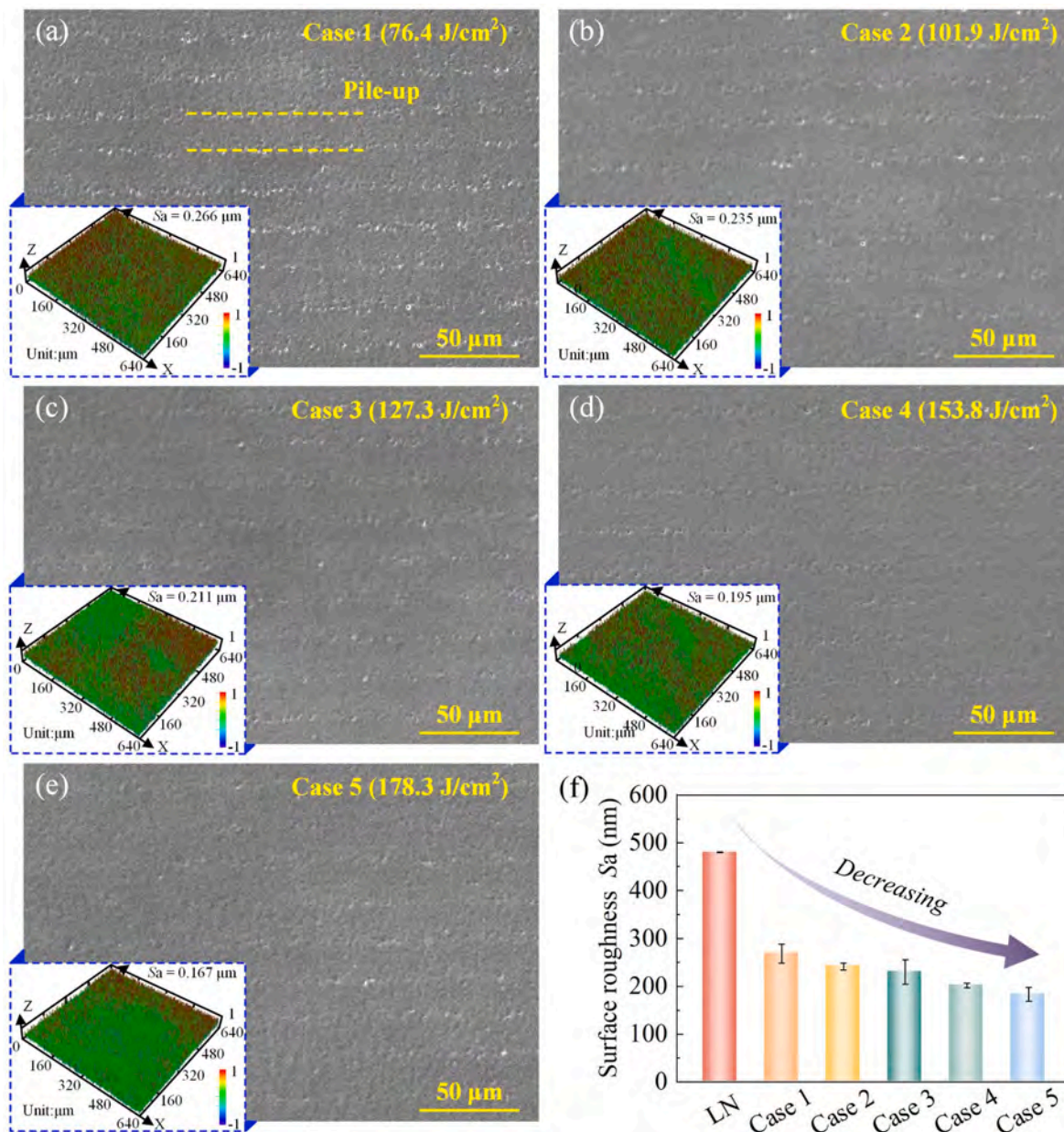
Fig. 2. SEM morphologies and corresponding 3D topographies of the LNed surface after laser shock flattening under different laser energy densities, corresponding to five test cases: (a) case 1, (b) case 2, (c) case 3, (d) case 4, and (e) case 5. (f) The surface roughness of the LNed MG and five test cases.

bumps and micro-pores are significantly reduced, which suggests that the laser shock flattening process is strongly dependent on the laser energy density used. To further quantitatively investigate the surface quality evolution induced by laser shock flattening, the surface roughness of the LNed MG and five test cases were captured, and the corresponding results are presented in Fig. 2(f). With the increase of laser energy density, the surface roughness value shows a gradual decreasing trend, and the maximum reduction is 61.87% (from 0.48 to 0.183 μm) achieved at a relatively high laser energy density of 178.3 J/cm². The reasons for this variation law is that when the laser energy density is relatively low, the micro-defects such as micro-bumps on the LNed MG surface are difficult to be removed, and thus the surface roughness of the LNed MG subjected to laser shock flattening is slightly reduced. As the laser energy density continues to increase to an appropriate range, the laser energy is applied uniformly to the LNed MG surface, resulting in a flatter surface. It is worth noting that the standard deviation of the surface roughness of five test cases is significantly higher than that of the

LNed surface. This phenomenon is mainly due to the presence of micro-bumps and micro-pores on the LNed surface, which make it absorb energy unevenly during the laser shock flattening process, resulting in unsatisfactory consistency in the surface quality of the five test cases. In light of the results presented in Fig. 2, it can be concluded that laser shock processing in an argon atmosphere is an effective strategy for achieving surface flattening of the LNed MG, and the resulting surface quality is dominated by the laser energy density used.

Fig. 3(a) illustrates the statistical results of hardness for the as-cast surface, LNed MG, and five test cases. The hardness of the LNed MG is significantly higher than that of as-cast surface, confirming the LN-induced hardening phenomenon in the Zr-based MG. This can be attributed to the introduction of hard nitrided phases mainly consisting of Zr_3N_4 and Ti_4N_3. On the one hand, these crystalline phases, as secondary phases embedded in the MG substrate, can effectively impede the propagation of the main shear band and enhance the resistance of the MG to plastic deformation. On the other hand, the hardness of these
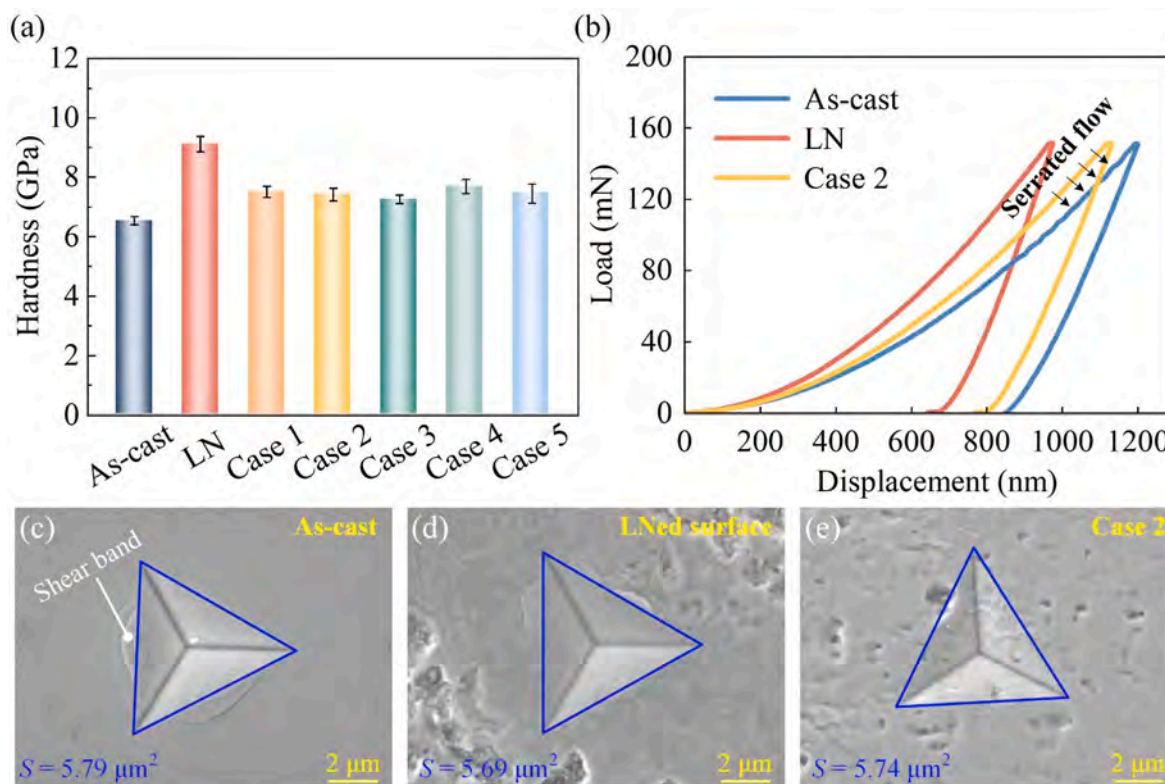
Fig. 3. (a) The statistical hardness results of as-cast MG, LNed MG and five test cases. (b) The representative load-displacement curves of as-cast MG, LNed MG and case 2. Representative morphologies of residual indents for (c) as-cast MG, (d) LNed MG, and (e) case 2.

crystalline phases is significantly higher than that of the MG substrate. The average hardness of the LNed regions treated by laser shock flattening with different laser energy densities fluctuates in the range of 7.25–7.69 GPa, which is lower than that of the LNed MG but still higher than that of the as-cast surface. This difference in hardness is further confirmed by the typical load-displacement curves illustrated in Fig. 3 (b), where the maximum penetration depth for case 2 is between that for LNed MG and as-cast MG. Since the variability in plastic deformation ability originates from the change in free volume, the above results imply that the free volume in LNed MG increases after laser shock flattening. It is worth noting significant serrated flows (also known as pop-in event) are observed on the load-displacement curve of the as-cast MG, whereas they are absent on the load-displacement curves of the LNed MG and case 2. The generation of serrated flows is usually caused by the nucleation and propagation of shear bands, which is confirmed by the SEM morphologies of residual indents presented in Fig. 3(c)–(e).

To confirm whether the nitrided layer remains on the LNed MG surface after laser shock flattening, the cross-section of case 2 was prepared by diamond wire cutting, and then mechanically ground and polished for microscopic morphological observations and elemental composition analyzis. Fig. 4(a) presents the cross-sectional morphology corresponding to case 2, where a laser affecting layer covered with a large number of cluster-like structures is clearly observed. Fig. 4(b) and (c) give the distribution of Zr and N elements along the marked line in Fig. 4(a), respectively. It is seen that the concentrations of Zr and N elements in the laser affecting layer are higher than those in the MG substrate, which confirms that the nitrided layer still exists on the

surface of LNed MG after laser shock flattening.

4. Conclusions

In summary, laser shock processing on LNed MG has been attempted with an aim of achieving surface flattening, and the dependence of the laser shock flattening process on the laser energy density has been systematically investigated. The experimental results revealed laser shock flattening could effectively reduce the surface roughness (Sa) of LNed MG, and higher laser energy density induce better surface quality, with a maximum reduction in surface roughness of 61.87% (from 0.48 to 0.183 μm) achieved at a relatively high laser energy density of 178.3 J/cm^2. The nanoindentation measurements results indicated that laser shock flattening resulted in a maximum reduction in the surface hardness of the LNed MG from 9.12 to 7.25 GPa, but it is still higher than that of the MG substrate (6.5 GPa). This study not only provides a fundamental understanding for surface quality and mechanical property evolution of LNed MG induced by laser shock flattening, but also benefits their engineering applications.

CRediT authorship contribution statement

Hu Huang: Writing – original draft, Resources, Investigation, Funding acquisition, Data curation, Conceptualization. **Puhong Xu:** Writing – original draft, Investigation, Data curation. **Bo Liu:** Investigation, Data curation. **Hong An:** Investigation. **Yongfeng Qian:** Writing – review & editing, Writing – original draft, Methodology, Investigation,
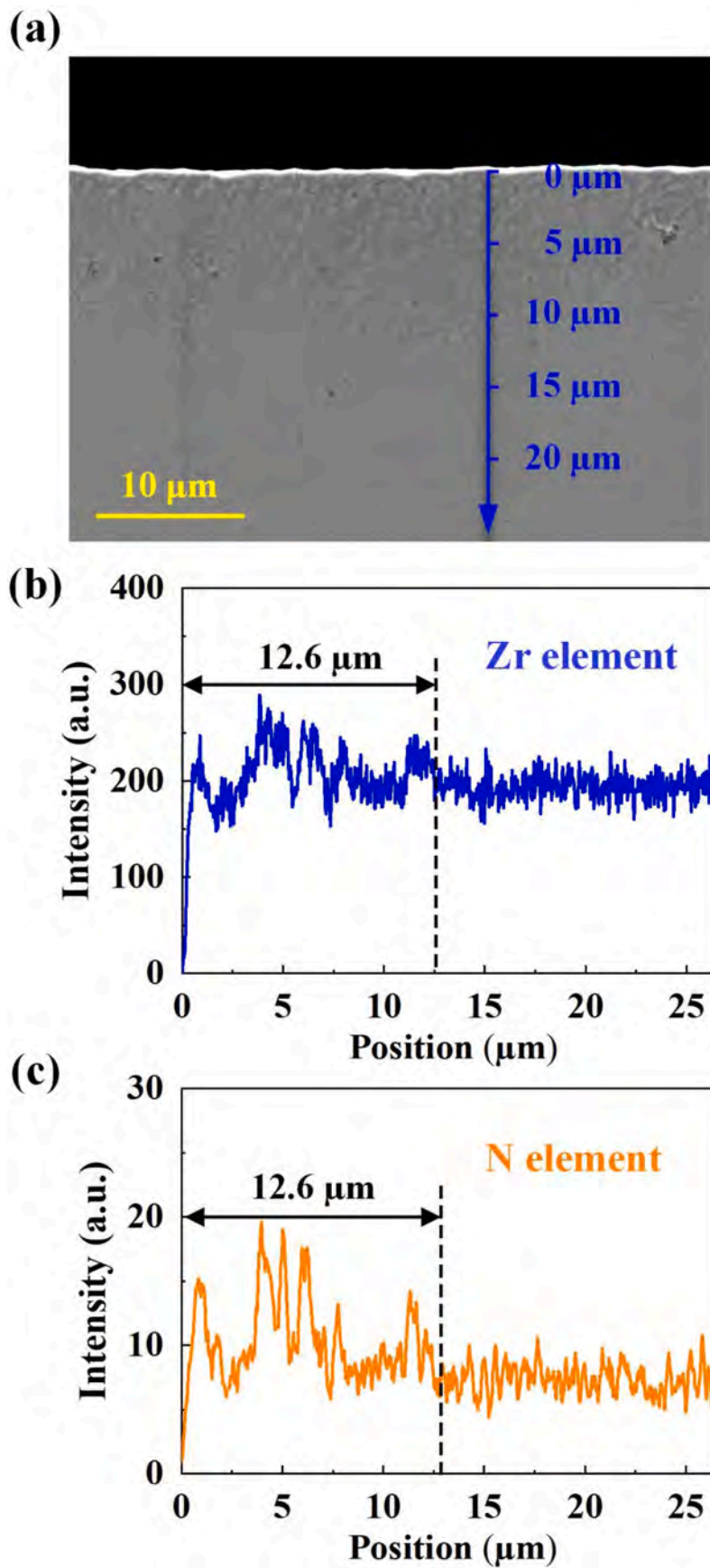
Fig. 4. (a) Cross-sectional morphology corresponding to case 2. (b) and (c) The distribution of Zr and N elements along the marked line in Fig. 4(a).

References

[1] I.K. Goetz, M. Kaplan, M. Hans, P. Ström, U. Jansson, B. Hjörvarsson, J. M. Schneider, Reactive metal additive manufacturing: surface near ZrN–metallic glass composite formation and mechanical properties, Addit. Manuf. 66 (2023) 103457.

[2] J. Hong, Y. Qian, L. Zhang, H. Huang, M. Jiang, J. Yan, Laser nitriding of Zr-based metallic glass: an investigation by orthogonal experiments, Surf. Coat. Technol. 424 (2021) 127657.

[3] Y. Qian, B. Liu, J. Hong, M. Jiang, Z. Zhang, L. Zhang, H. Huang, J. Yan, Simultaneous flattening and hardening of laser shock peened Zr-based metallic glass surface by nanosecond laser irradiation in a flowing nitrogen atmosphere, J. Mater. Process. Technol. 326 (2024) 118313.

[4] Y. Qian, M. Jiang, Z. Zhang, H. Huang, J. Hong, J. Yan, Microstructures and mechanical properties of Zr-based metallic glass ablated by nanosecond pulsed laser in various gas atmospheres, J. Alloys Compd. 901 (2022) 163717.

[5] J. Mu, T. Sun, C.L.A. Leung, J.P. Oliveira, Y. Wu, H. Wang, H. Wang, Application of electrochemical polishing in surface treatment of additively manufactured structures: a review, Prog. Mater. Sci. 136 (2023) 101109.

[6] A. Sebastian, F. Zhang, A. Dodda, D. May-Rawding, H. Liu, T. Zhang, M. Terrones, S. Das, Electrochemical polishing of two-dimensional materials, ACS Nano 13 (1) (2019) 78–86.

[7] C. Ding, M.-y. Liu, S.-z. Wan, Z.-y. Cai, L.-j. Yuan, R. Wang, P. Zheng, The sustainable treatment of chemical polishing wastewater under low-carbon economy: pollutants removal, resource recovery and energy generation, J. Clean. Prod. 414 (2023) 137469.

[8] L.R. Skubal, D.R. Walters, Chemical polishing of aluminum coupons in support of vacuum chambers, Vacuum 96 (2013) 1–6.

[9] P.K. Baghel, V. Mishra, R. Kumar, G.S. Khan, Ultrasonic vibration–assisted magnetorheological hybrid finishing process for glass optics, Int. J. Adv. Manuf. Technol. 125 (5) (2023) 2265–2276.

[10] T. Yu, J. An, X. Yang, X. Bian, J. Zhao, The study of ultrasonic vibration assisted polishing optical glass lens with ultrasonic atomizing liquid, J. Manuf. Process. 34 (2018) 389–400.

[11] H. Luo, S. Yin, G. Zhang, C. Liu, Q. Tang, M. Guo, Optimized pre-thinning procedures of ion-beam thinning for TEM sample preparation by magnetorheological polishing, Ultramicroscopy 181 (2017) 165–172.

[12] D. Ma, M. Ji, H. Yi, Q. Wang, F. Fan, B. Feng, M. Zheng, Y. Chen, H. Duan, Pushing the thinness limit of silver films for flexible optoelectronic devices via ion-beam thinning-back process, Nat. Commun. 15 (1) (2024) 2248.

[13] W. Deng, C. Wang, H. Lu, X. Meng, Z. Wang, J. Lv, K. Luo, J. Lu, Progressive developments, challenges and future trends in laser shock peening of metallic materials and alloys: a comprehensive review, Int. J. Mach. Tool Manufact. 191 (2023) 104061.

[14] B. Dhakal, S. Swaroop, Review: laser shock peening as post welding treatment technique, J. Manuf. Process. 32 (2018) 721–733.

[15] Y. Li, K. Zhang, Y. Wang, W. Tang, Y. Zhang, B. Wei, Z. Hu, Abnormal softening of Ti-metallic glasses during nanosecond laser shock peening, Mater. Sci. Eng. A 773 (2020) 138844.

[16] Y.V. A, M. Vadani, B. Karan, A. Bhakar, S. Rai, N. Maharjan, A. Bhowmik, Investigation of surface structural modifications caused by the influence of the ablative layer in Inconel718 Ni-base superalloy through laser shock peening, Mater. Lett. 354 (2024) 135332.

[17] M.V. Nataraj, S. Swaroop, Effects of power density on residual stress and microstructural behavior of Ti-2.5Cu alloy by laser shock peening without coating, Vacuum 213 (2023) 112078.

[18] Y. Haifeng, X. Fei, W. Yan, W. Le, L. Hao, H. Jingbin, Manufacturing profile-free copper foil using laser shock flattening, Int. J. Mach. Tool Manufact. 152 (2020) 103542.

[19] A.J. Bischoff, A. Arabi-Hashemi, M. Ehrhardt, P. Lorenz, K. Zimmer, S.G. Mayr, Shock wave induced martensitic transformations and morphology changes in Fe-Pd ferromagnetic shape memory alloy thin films, Appl. Phys. Lett. 108 (15) (2016) 151901.

[20] C. Qiu, C. Panwisawas, M. Ward, H.C. Basoalto, J.W. Brooks, M.M. Attallah, On the role of melt flow into the surface structure and porosity development during selective laser melting, Acta Mater. 96 (2015) 72–79.